Journal of ELECTRONIC MATERIALS, Vol. 44, No. 8, 2015
DOI: 10.1007/s11664-015-3734-4

Effect of InP Doping on the Phase Transition of Thin GeSbTe Films

KI SU BANG,[1] YONG JUN OH,[1] and SEUNG-YUN LEE[1,2]

1.—Department of Applied Materials Engineering, Hanbat National University, Daejeon 305-719, Korea. 2.—e-mail: sy_lee@hanbat.ac.kr

We report the crystallization and phase-transition behavior of GeSbTe thin films doped with indium phosphorus (InP). Pure GeSbTe thin films and InP-doped GeSbTe thin films were prepared by use of an rf magnetron sputtering method. After thermal annealing, electrical and optical changes in the thin films were observed. Sheet resistance and reflectance measurements revealed that InP doping suppresses crystallization of GeSbTe. X-ray diffraction analysis confirmed that addition of In and P atoms inhibits the phase transition from face-centered cubic to hexagonal closed-packed. Nucleation of the doped GeSbTe thin films was delayed at an annealing temperature of 100°C; after thermal annealing, neither segregation nor formation of a secondary phase occurred. These results indicate that InP doping improves the amorphous stability of GeSbTe thin films. It is believed this enhanced amorphous stability is a result of the formation of multiple, strong crosslinks by the In and P atoms.

Key words: Chalcogenides, GeSbTe, InP, phase transition, crystallization, phase change memory

INTRODUCTION

Chalcogenides are among the most important amorphous semiconductors, with numerous applications in solid-state electronic and photovoltaic devices, for example phase-change memory and solar cells. Some chalcogenides can reversibly switch between crystalline and amorphous states, depending on energy input, and their electrical resistivity and optical reflectance change with the phase transition.[1–4] Among chalcogenide compounds, GeSbTe is the best known phase-change material (PCM) and is commonly used in phase-change memory[5,6] and for optical storage media.[7]

Much research has been conducted on doping of PCMs with specific materials (for example nitrogen,[8,9] oxygen,[10,11] silicon,[12,13] silver,[14] bismuth,[15] indium,[16] cerium,[17] and dielectric compounds[18,19]). Because the properties of PCMs can be adjusted by use of different doping processes, it is possible to create a range of PCMs with appropriate improved characteristics. For instance, on addition of some elements,[8,12] the amorphous stability of PCMs can be enhanced and the resistivity of the crystallized PCMs can be increased. This results in such advantages as enhanced amorphous stability, which leads to retention of more data.[20] It also increases resistivity, which reduces the programming current required for the phase change induced by resistive Joule heating.[21] Moreover, the doping process enables the creation of unique functions for PCMs. If the stability of the amorphous state is further increased by doping with impurities, a PCM for which memory switching behavior is usually observed can be converted into a threshold-switching material. This chalcogenide material can then be used as an active layer, not in phase change memory, but in such Ovonic threshold switching devices as selectors[22] and programmable switches.[23] A variety of methods, for example, introduction of new device structures, is used to improve performance, resulting in novel applications of chalcogenide-based devices. PCM doping is regarded as one of the most fundamental approaches to optimization of device characteristics.

In this paper we report the effects of InP doping on the phase transition characteristics of $Ge_2Sb_2Te_5$

(Received October 30, 2014; accepted March 6, 2015; published online March 26, 2015)

(GST) films. Both indium and phosphorus are known to significantly affect the network connectivity of tellurium-based chalcogenide alloys.[24–26] Also, unlike elemental phosphorus, InP is highly stable under normal laboratory conditions. In addition, during sputtering of alloys, most sputtered species are in their atomic form.[27] Because indium and phosphorus atoms, rather than InP clusters, are likely to be included in GST films when InP is sputtered, we selected InP as a dopant source material, and were able to incorporate indium and phosphorus into GST films during rf magnetron sputtering deposition.

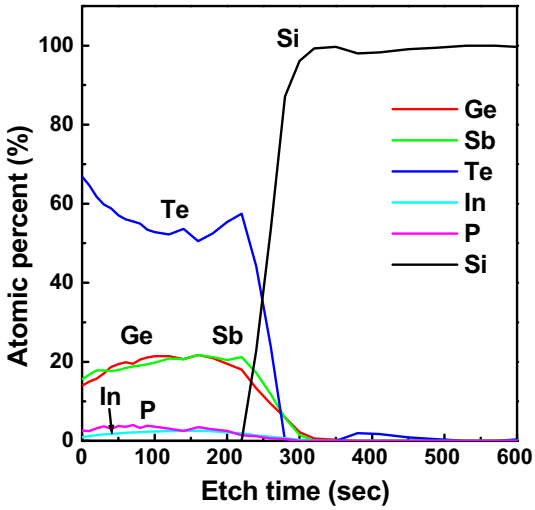

Fig. 1. AES depth profiles of doped GST thin film.

EXPERIMENTAL

By use of an rf magnetron method, pure GST and InP-doped GST thin films were deposited at room temperature. A two-inch $Ge_2Sb_5Te_5$ target on which a piece of InP single-crystal wafer was attached (i.e. the GST-InP target) was used for preparing doped GST films. *p*-Type Si ⟨100⟩ wafers, serving as substrate, were cut into approximately 2.0 × 2.0 cm^2 squares and were successively cleaned in acetone, trichloroethylene, ethyl alcohol, and distilled water, each time for 10 min. The specimens were placed in the sputtering chamber, and pre-sputtering was performed for 10 min before film deposition. To stabilize the plasma, sputtering power was maintained at 50 W, and the Ar flow was held constant at 20 sccm. During sputtering, the process pressure was 1.3 × 10^{-3} torr. The thicknesses of the as-deposited GST and InP-doped GST films ranged from 24 nm to 30 nm. However, thicker films were used to evaluate the effect of InP doping on sheet resistance. After sputter deposition, thermal annealing was performed in an Ar atmosphere at 1 atm. The rates of heating and cooling were 50°/min and 1–5°/min (furnace cooling), respectively, and the annealing temperature, which ranged from 100°C to 400°C, was maintained constant over a period of 20 min.

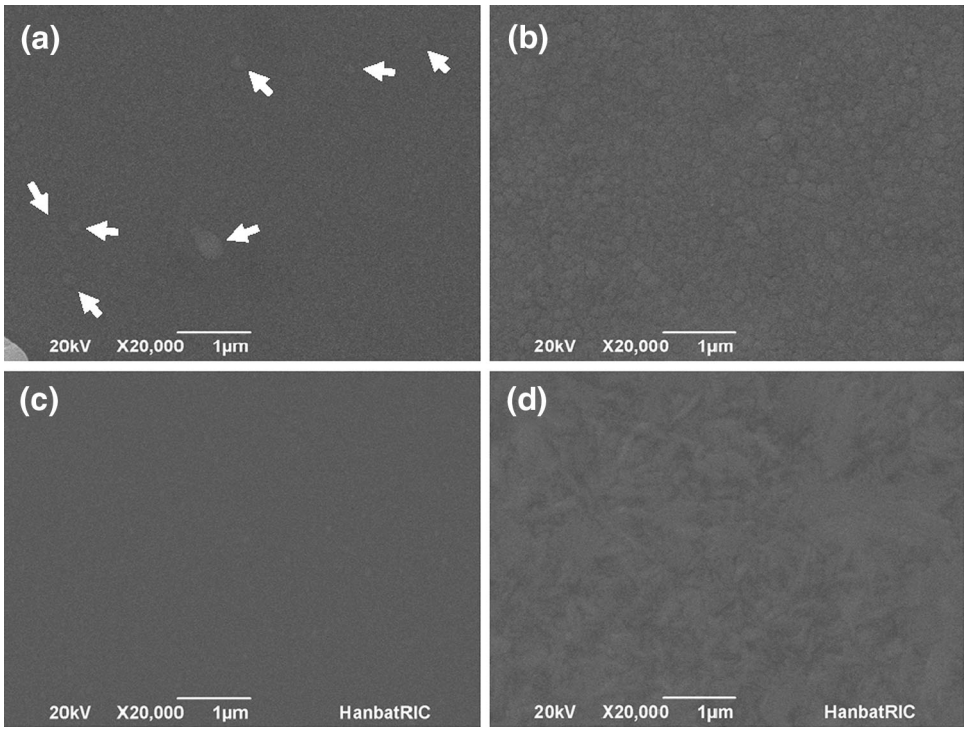

Fig. 2. Plan-view SEM images of GST thin films annealed at (a) 300°C and (b) 400°C, and of doped GST thin films annealed at (c) 300°C and (d) 400°C. The arrows in (a) indicate round grains with thermal grooves.

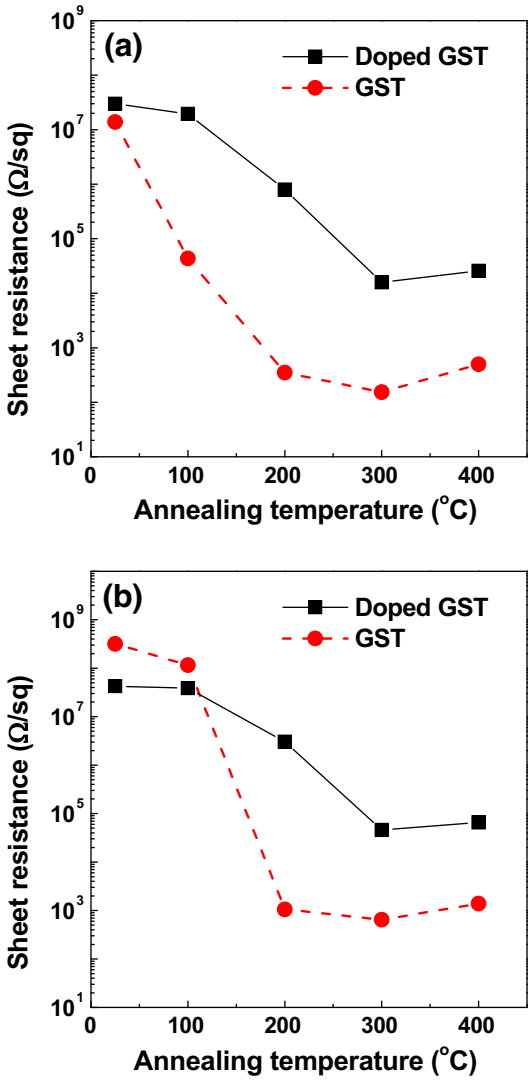

Fig. 3. (a) Sheet resistance changes for 30 nm-thick GST and for 24 nm-thick doped GST thin films annealed at different temperatures. (b) Sheet resistance changes for 185 nm-thick GST and 190 nm-thick doped GST thin films annealed at different temperatures.

Film thickness was measured by use of a stylus profilometer, and the atomic concentrations of each element in the doped GST film were determined by use of Auger electron spectroscopy (AES). Sheet resistance was determined by use of a linear four-point probe method. Crystallization temperatures of the pure GST and doped GST films were estimated by use of differential scanning calorimetry (DSC). The reflectance of the films was measured by use of an ultraviolet–visible spectrophotometer. The crystalline phases of the pure GST and doped GST films were determined by use of x-ray diffraction (XRD) using Seemann–Bohlin geometry. The surface morphology and internal microstructure of the films were examined by use of scanning electron microscopy (SEM) and transmission electron microscopy (TEM).

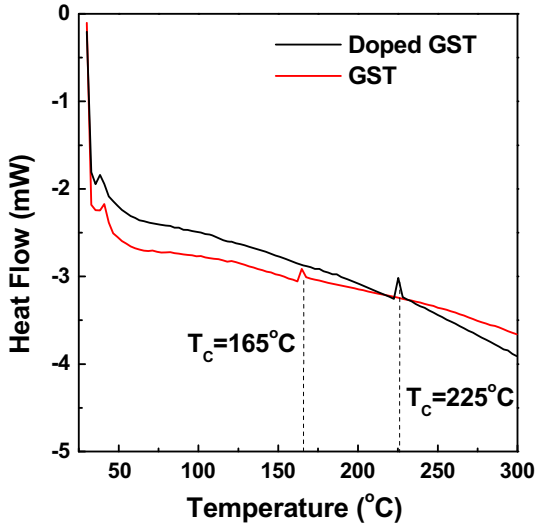

Fig. 4. DSC thermogram of GST and doped GST thin films (heating rate 10°/min).

RESULTS AND DISCUSSION

The AES depth profiles of the doped GST film clearly show that In and P atoms are distributed throughout the film (Fig. 1). In and P content ranged from 1.8 at.% to 4.0 at.% and the atomic percentage ratio of In to P in the middle of the doped GST film was approximately 1.0. Although there were significant fluctuations in the concentrations of Ge, Sb and Te near the surface and at the interface between the doped GST film and the Si substrate, those in the middle of the doped GST film were approximately uniform, and the Ge–Sb–Te atomic percentage ratio was 22:22:53. The AES results imply that rf sputtering from the GST-InP target, formed by attachment, can furnish a uniformly doped GST film.

Figure 2 shows plan-view SEM images of pure GST and doped GST films, annealed at 300°C and 400°C. The surfaces of the as-deposited films were very smooth (images not shown), but those of the films annealed at 400°C were comparatively rough. This surface roughening of the films at elevated temperature is believed to be closely related to phase transition from an amorphous to a crystalline state. Morphological changes of film surface are caused by thermal grooving at grain boundaries.[28] Therefore, the flat surface of the as-deposited film, which can be amorphous, becomes unstable as crystallization proceeds. The surface of the pure GST film becomes irregular at an annealing temperature of 300°C, whereas the surface of the doped GST film becomes irregular at the higher temperature, 400°C. Round grains with thermal grooves were sparsely distributed in the pure GST film whereas the surface of the doped GST film remained flat after annealing at 300°C, as shown in Fig. 2a and c. Therefore, it is probable that InP doping affects the crystallization process and has a

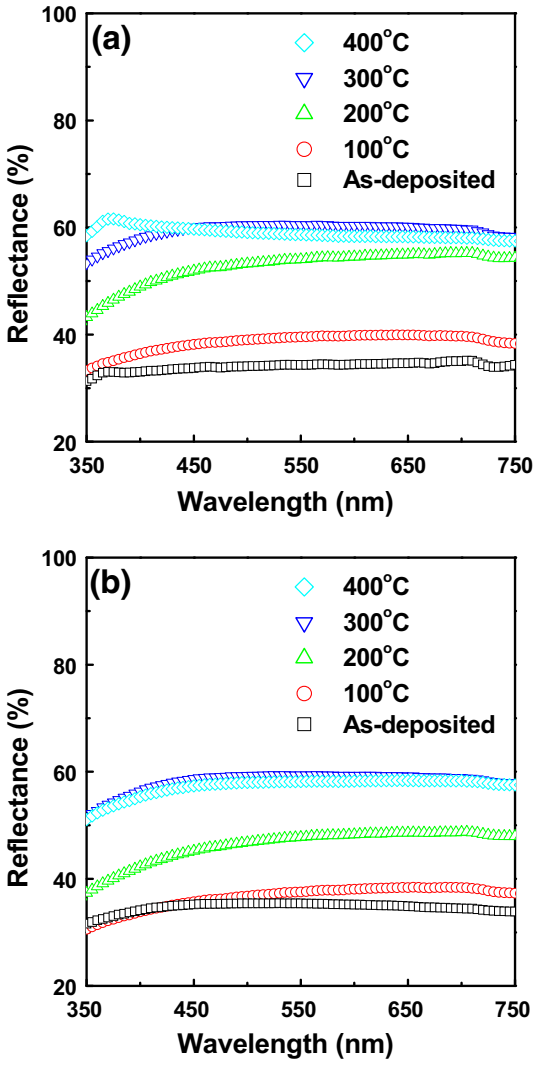

Fig. 5. Reflectance spectra of (a) GST thin films, and (b) doped GST thin films annealed at different temperatures.

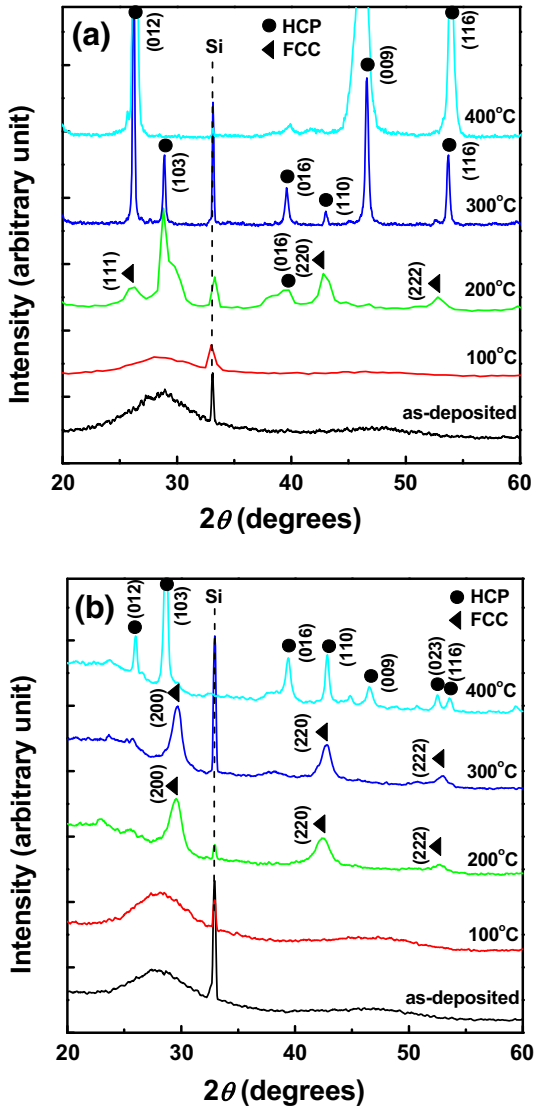

Fig. 6. X-ray diffraction patterns of (a) GST thin films, and (b) doped GST thin films annealed at different temperatures.

suppressive effect on surface morphology changes within the GST film.

Figure 3a shows sheet resistance changes for 30 nm-thick GST and 24 nm-thick doped GST films with increasing annealing temperature. As the annealing temperature increases, the sheet resistances of both films decrease then saturate. However, the resistance and temperature range corresponding to saturation are substantially different for the two types of film. The sheet resistance of pure GST and doped GST films saturates at approximately 200°C and 300°C, respectively. The saturated value of sheet resistance for the doped GST film is approximately two orders of magnitude larger than that of the pure GST film. It is worthy of note that the same tendency was observed for thicker films (185–190 nm), as shown in Fig. 3b, which indicates that the effect of InP doping is consistent, irrespective of film thickness. According to other reports,[29,30] the resistivity of the amorphous GST film decreases substantially with increasing temperature, as a result of crystallization. Thus, the decrease of the sheet resistance is attributed to the phase transition of the GST film from an amorphous to a crystalline state. The sheet resistance of doped GST films leveled off at a higher temperature than that of the pure GST film, suggesting that In and P atoms added to the GST film inhibit crystallization. The sheet resistance was slightly higher at 400°C than at 300°C. The reason for this is unclear, but it is likely to be associated with oxidation as a result of residual oxygen in the annealing chamber. DSC analysis was performed for quantitative comparison of crystallization temperatures; the results are shown in Fig. 4. The DSC thermogram clearly shows that the pure GST and doped GST films crystallize at 165°C and 225°C, respectively. This supports the idea that InP doping

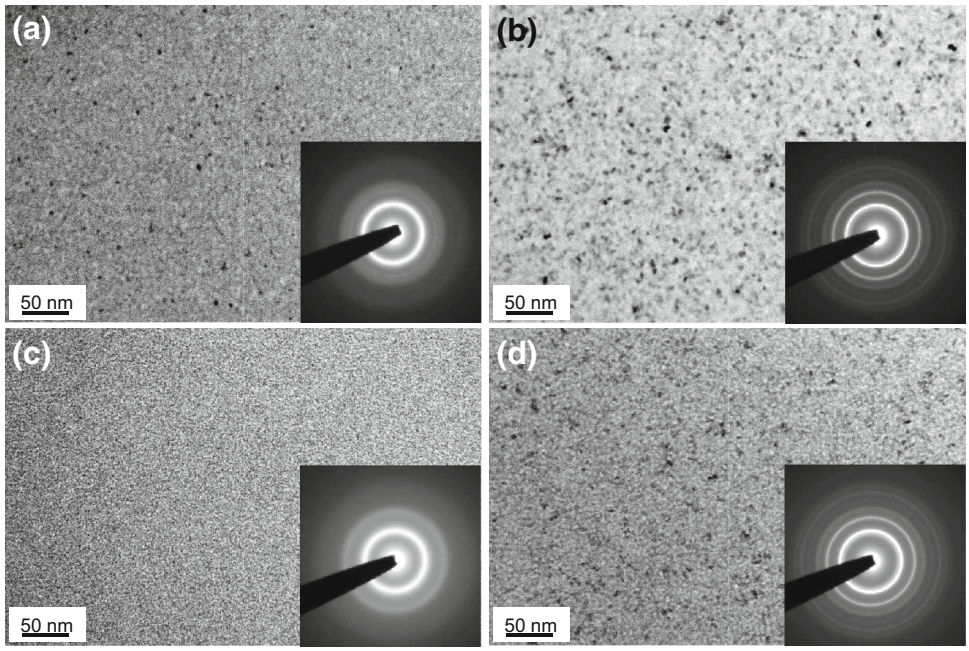

Fig. 7. Plan-view TEM images with electron diffraction patterns of GST thin films annealed at (a) 100°C and (b) 300°C, and of doped GST thin films annealed at (c) 100°C and (d) 300°C.

leads to a higher crystallization temperature for the GST film.

The reflectance spectra of GST and doped GST films also reveal that InP doping suppresses crystallization of GST films (Fig. 5). The reflectance of the two types of film varied in the same manner as for increasing annealing temperature, although the detailed dependence of reflectance was slightly different. Compared with the pure GST film, the increase in reflectance of the doped GST film was less pronounced after annealing at 100°C and 200°C. Because the reflectance of the pure GST film is proportional to the volume fraction of crystalline GST,[31] the reflectance depends on the extent of crystallization. Therefore, the gradual increase in the reflectance of the doped GST film implies that crystallization is hindered by addition of In and P atoms.

The detailed transition behavior of the pure GST and doped GST films was confirmed by results from XRD measurements (Fig. 6). Whereas typical XRD patterns of an amorphous structure were observed for the as-deposited films, different phases were identified in films post-annealed at 200°C or 300°C. Mixed phases of face-centered cubic (FCC) and hexagonal closed-packed (HCP) crystalline structures were present in the GST film annealed at 200°C; at 300°C, however, only the HCP phase remained (Fig. 6a). Unlike the pure GST film, the FCC phase was identified in doped GST films annealed at 200°C and 300°C (Fig. 6b). A single HCP phase was present in both types of film annealed at 400°C. It is well known that GST films undergo phase transitions from amorphous to FCC (140–250°C) and from FCC to HCP (230–350°C).[32,33] Thus, it is evident that InP doping increases the transition temperature from FCC to HCP from approximately 200°C to over 300°C. DSC analysis, in contrast, indicated that the crystallization temperature of the doped GST film was approximately 225°C. However, the FCC phase appeared in the doped GST film after annealing at 200°C. The discrepancy is attributed to the different heating methods used for DSC and XRD measurements. Choi et al.[33] reported that the crystallization temperature of GST film increases substantially with increasing rate of temperature rise. Whereas DSC analysis was performed over a period with gradual heating, XRD patterns were obtained after annealing for 20 min. This resulted in formation of FCC phases at a temperature lower than the crystallization temperature measured by DSC.

The effect of InP doping on suppression of phase transition was further supported by TEM analysis. Small grains, ranging from 5 nm to 10 nm, were frequently observed in pure GST films annealed at 100°C (Fig. 7a). No crystallites were observed in doped GST films annealed at the same temperature, however (Fig. 7c). The different crystallization behavior of the two types of film is clearly apparent from the insets of Fig. 7a and c. The diffuse electron diffraction pattern of the inset of Fig. 7c implies that the microstructure of the doped GST film annealed at 100°C is either amorphous or composed of extremely small grains, and also that In and P suppress nucleation. Also, for pure GST and doped GST films annealed at 300°C, the microstructure is

different. Well-distinguished grains are often observed in GST films, and the grain size is larger than that of the doped GST film (Fig. 7b and d). This TEM observation indicates that InP doping suppresses both the nucleation and grain growth processes in GST films.

The reason for these effects of InP doping might be closely related to the effect of In and P atoms on chalcogenide alloys. When the connectivity or rigidity of the structural network of tellurium-based chalcogenide compounds is high, their crystallization becomes difficult. Indium atoms increase the network connectivity by fourfold coordination with Te. As a result, formation of Te metallic crystals is inhibited, and the stability of the amorphous state is enhanced.[24] Furthermore, addition of In to chalcogenide replaces Te–Te bonds with In–Te bonds, resulting in a more rigid network.[25] An increase in network connectivity and suppression of crystallization have been reported as a result of doping with such VA elements as As and P, for which the coordination number is larger than for group VIA chalcogens.[26] Thus, the effect of InP doping is attributed to suppression of nucleation, caused by a large number of strong crosslinks between constituent atoms. This postulate is also supported by the fact that no segregation or formation of secondary phase occurs in doped thin films.

The effect of In and P atoms is distinctly different from that of such dopants as N, O, Si, and In, which accumulate at grain boundaries or segregate and then restrict grain growth.[8–13,16] From the perspective of device reliability, because In and P atoms completely dissolve in the GST matrix and do not induce formation of a secondary phase, InP is believed to be superior to the other dopants. In repetitive operations, however, the performance of devices can be degraded by doping of films, because of segregation of phases or because of gas molecules trapped by immiscible dopants.[9]

CONCLUSIONS

InP-doped GST thin films were prepared by rf magnetron sputtering, and their electrical and optical characteristics were then compared with those of pure GST thin films. The sheet resistance of the doped thin film decreased with increasing annealing temperature, and reached its minimum at a temperature of 100°C higher than that of pure GST film. Compared with the pure GST, the reflectance of the doped thin film was increased slightly by annealing at 100°C and 200°C. X-ray diffraction and TEM analysis showed that InP doping suppresses nucleation of the amorphous phase and the phase transition from FCC to HCP in the GST thin film. No segregation or formation of a secondary phase occurred in the doped thin film, so the effect of InP doping is attributed to the intrinsic nature of In and P atoms in enhancing the network connectivity and rigidity of tellurium-based chalcogenide compounds. This manipulation of the properties of the phase-change material suggests an effective means of producing GST-based electronic and optical devices with high performance and multiple functions.

ACKNOWLEDGEMENTS

This research was supported by the Basic Science Research Program through the National Research Foundation of Korea, funded by the Ministry of Education NRF-2013R1A1A2058709.

REFERENCES

1. M. Nardone, M. Simon, I.V. Karpov, and V.G. Karpov, *J. Appl. Phys.* 112, 071101 (2012).
2. N. Yamada, *MRS Bull.* 21, 48 (1996).
3. K. Ren, F. Rao, Z. Song, S. Lv, Y. Cheng, L. Wu, C. Peng, X. Zhou, M. Xia, B. Liu, and S. Feng, *Appl. Phys. Lett.* 100, 052105 (2012).
4. S.R. Ovshinsky, *Phys. Rev. Lett.* 21, 1450 (1968).
5. J.-B. Park, G.-S. Park, H.-S. Baik, J.-H. Lee, H. Jeong, and K. Kim, *J. Electrochem. Soc.* 154, H139 (2007).
6. Q. Wang, H.J. Sun, J.J. Zhang, X.H. Xu, and X.S. Miao, *J. Electron. Mater.* 41, 3417 (2012).
7. A.V. Kolobov, J. Tominaga, and J. Mater, *Sci.-Mater. El.* 14, 677 (2003).
8. H. Horii, J.H. Yi, J.H. Park, Y.H. Ha, I.G. Baek, S.O. Park, Y.N. Hwang, S.H. Lee, Y.T. Kim, K.H. Lee, U.-I. Chung, and J.T. Moon (Symposium on VLSI Technology Digest of Technical Papers, 2003), pp. 177.
9. K.-H. Kim, D.-J. Yun, Y.-K. Kyoung, D.-E. Yu, and S.-J. Choi, *J. Electron. Mater.* 43, 3082 (2014).
10. M.H. Jang, S.J. Park, D.H. Lim, S.J. Park, and M.H. Cho, *Appl. Phys. Lett.* 96, 092108 (2010).
11. T.H. Jeong, H. Seo, K.L. Lee, S.M. Choi, S.J. Kim, and S.Y. Kim, *Jpn. J. Appl. Phys.* 40, 1609 (2001).
12. Y. Jiang, L. Xu, J. Chen, R. Zhang, W. Su, Y. Yu, Z. Ma, and J. Xu, *Phys. Status Solidi A* 210, 2231 (2013).
13. L. Tong, L. Xu, Y. Jiang, F. Yang, L. Geng, J. Xu, W. Su, Z. Ma, and K. Chen, *J. Non-Cryst. Solids* 358, 2402 (2012).
14. K.H. Song, S.W. Kim, J.H. Seo, and H.Y. Lee, *J. Appl. Phys.* 104, 103516 (2008).
15. K. Wang, D. Wamwangi, S. Ziegler, C. Steimer, and M. Wuttig, *J. Appl. Phys.* 96, 5557 (2004).
16. K. Wang, C. Steimer, D. Wamwangi, S. Ziegler, and M. Wuttig, *Appl. Phys. A* 80, 1611 (2005).
17. Y.J. Huang, M.C. Tsai, C.H. Wang, and T.E. Hsieh, *Thin Solid Films* 520, 3692 (2012).
18. S.W. Ryu, Y.B. Ahn, J.H. Lee, and H.J. Kim, *J. Semicond. Technol. Sci.* 11, 146 (2011).
19. T. Morikawa, K. Akita, T. Ohyanagi, M. Kitamura, M. Kinoshita, M. Tai, and N. Takaura (IEEE International Electron Devices Meeting (IEDM), 2012), pp. 31.4.1–31.4.4.
20. A.M. Mio, G. D'Arrigo, E. Carria, C. Bongiorno, S. Rossini, C. Spinella, M.G. Grimaldi, and E. Rimini, *Electrochem. Solid-State Lett.* 15, H105 (2012).
21. Y. Yin and S. Hosaka, *Jpn. J. Appl. Phys.* 51, 104202 (2012).
22. M. Anbarasu, M. Wimmer, G. Bruns, M. Salinga, and M. Wuttig, *Appl. Phys. Lett.* 100, 143505 (2012).
23. T. Lowrey, W. Parkinson, and G. Wicker, US Patent US 8379439 B2 (2013).
24. Z. Yang and P. Lucasw, *J. Am. Ceram. Soc.* 92, 2920 (2009).
25. N. Manikandan and S. Asokan, *J. Phys. Condens. Matter* 19, 376104 (2007).
26. S. Prakash, S. Asokan, and D.B. Ghare, *IEEE Electron. Dev. Lett.* 18, 45 (1997).
27. D.A. Glocker and S.I. Shah, *Handbook of Thin Film Process Technology* (London: Institute of Physics, 1995), p. A3.0.11.

28. S.-Y. Lee, S.-H. Choi, and C.-O. Park, *Thin Solid Films* 359, 261 (2000).
29. I. Friedrich, V. Weidenhof, W. Njoroge, P. Franz, and M. Wuttig, *J. Appl. Phys.* 87, 4130 (2000).
30. S.O. Ryu, S.M. Yoon, K.J. Choi, N.Y. Lee, Y.S. Park, S.Y. Lee, B.G. Yu, J.B. Park, and W.C. Shin, *J. Electrochem. Soc.* 153, G234 (2006).
31. S. Raoux and M. Wuttig, *Phase-change materials Science and Applications* (New York: Spring, 2009), p. 187.
32. N. Kato, I. Konomi, Y. Seno, and T. Motohiro, *Appl. Surf. Sci.* 244, 281 (2005).
33. Y. Choi, M. Jung, and Y.-K. Lee, *Electrochem. Solid-State Lett.* 12, F17 (2009).